Robotica: (2020) volume 38, pp. 669–683. © Cambridge University Press 2019
doi:10.1017/S026357471900095X

A Unified Architecture for Physical and Ergonomic Human–Robot Collaboration

Federica Ferraguti†*, Renzo Villa‡, Chiara Talignani Landi†, Andrea Maria Zanchettin‡, Paolo Rocco‡ and Cristian Secchi†

†*Università di Modena e Reggio Emilia, Dipartimento di Scienze e Metodi dell'Ingegneria, via Amendola 2, 42122 - Reggio Emilia, Italy.*
E-mails: chiara.talignanilandi@unimore.it, cristian.secchi@unimore.it
‡*Politecnico di Milano, Dipartimento di Elettronica, Informazione e Bioingegneria, Piazza L. Da Vinci 32, 20133 - Milano, Italy.*
E-mails: renzo.villa@polimi.it, andreamaria.zanchettin@polimi.it, paolo.rocco@polimi.it

(Accepted May 25, 2019. First published online: June 19, 2019)

SUMMARY
Industrial applications that involve working on and moving a heavy load or that constrain the operator to work in uncomfortable positions can take advantage of the assistance of a robotic assistant. In this paper, we propose an architecture for an ergonomic human–robot co-manipulation of objects of various shapes and weight. The object is carried by the robot and, thanks to an ergonomic planner, is positioned in the most comfortable way for the user. Furthermore, thanks to an admittance control with payload compensation, the user can easily adjust the position of the object for working on different parts of it. The proposed architecture is experimentally validated in a robotic cell including an ABB industrial robot.

KEYWORDS: Human–Robot interaction; Control of robotic systems; Man–Machine system.

1. Introduction

Human–robot collaboration is a fast growing field of robotics, paving the way to a scenario where robots can be used in unstructured environments cooperating closely with humans for fulfilling a task (see, e.g., ref. [1]), or at least sharing the same workplace as in ref. [2]. As a consequence, humans and robots work close together in the manufacturing environment.[3,4] As flexibility requirements continue to increase, the optimal degree of automation will turn out to be less than 100%, and the role of the human worker remains important.[5,6] However, all the applications that are currently executed by a human operator with a big effort and in uncomfortable positions (e.g., riveting bulky pieces and welding hardly reachable parts) can tremendously benefit of a robotic collaborator. In this paper, we consider a scenario where a human has to perform operations on a variety of objects, including heavy or bulky ones. In this case, the operator is required to handle possibly heavy payloads and/or to work in uncomfortable positions. On the other hand, managing each kind of payload is an easy task for a robot that, however, lacks the skills to perform complex tasks where the experience of the user is required. Thus, the capabilities of the robot can be combined with the user's experience and skills to create a human–robot collaborative system, where the robot carries and holds the payload, while the user manipulates it and performs the required operations.

Safety and ergonomics are of paramount importance for this kind of applications. Thus, it is necessary to exploit control strategies that guarantee a compliant behavior of the robot, to ensure a safe and natural behavior. Admittance control[7] has been successfully exploited for making an industrial robot

* Corresponding author. E-mail: federica.ferraguti@unimore.it

https://doi.org/10.1017/S026357471900095X Published online by Cambridge University Press

compliant. For example, admittance control has been exploited in ref. [8] to develop a walk-through programming scheme for manual guidance of the robot, while in ref. [9] it has been adopted to provide a very intuitive human–robot interaction.

Industrial applications involving human–robot co-manipulation have been extensively studied in the literature. In particular, in ref. [10] several control strategies to allow the human and a robotic manipulator to co-manipulate heavy and bulky objects have been proposed. Since in these tasks the robot has to carry loads that could be characterized by high inertia, the static and dynamic components of the payload need to be compensated, as suggested in ref. [11]. The compensation can then be integrated in the admittance control as proposed in ref. [12].

More recently, the attention has been more focused on personalizing the interaction, for example, to account for physiological differences of individuals[13] or to predict human intent based on skeletal pose.[14] Recently, in ref. [15], a feedback interaction controller has been proposed in order to reduce the static joint overloading of the human worker during co-manipulation. However, if the object to be co-manipulated is heavy and bulky, ergonomics and a good posture of the human operator, who has to be able to handle the object comfortably, become very important issues. In essence, ergonomics is the science that studies the performance and the well-being of the human worker in relation to the purposes of his/her operations, the equipment, and the working environment. This translates in the design of products and/or processes that use the capabilities of an individual, taking into account his/her physiological and psycho-intellectual needs. The ergonomic issues have long been known,[16] and recently they have been addressed in robotic fields such as, for example, surgical robotics.[17] In the last years, ergonomics issues are also being considered related to collaborative robots.[18]

Despite the rich literature in ergonomics and in safe physical human–robot interaction, to the best of the authors' knowledge the problem of developing a cooperative system combining these two features for industrial co-manipulation has not been fully addressed yet. Indeed, in order to be applicable in realistic scenarios, a quantitative assessment of the operator posture, possibly minimizing the adoption of sophisticated and expensive sensors, has to be adopted when designing the co-manipulation task.

The goal of this paper is to develop a safe and ergonomic control architecture for the co-manipulation of objects of various shapes and weight. We consider a scenario where the robot assists the worker, carrying at the end-effector an object over which the human is supposed to perform some operations. Thanks to an ergonomic motion planner, the robot can adjust the position of the object in order to optimize the ergonomics, allowing the operator to take the most comfortable working posture. An admittance control with payload compensation allows the user to safely and easily manipulate the object carried by the robot. The ergonomic planner and the admittance control are used in a mutually exclusive way. The planner is exploited for moving the part from the starting position (e.g., a pallet) to the human, while the admittance control is used for allowing the operator to easily manipulate the part while working on it. In order to make the system even easier to use, the switch between the two working modes is implemented by means of a force password which saves the user from taking care of external interfaces.

In a nutshell, the main contribution of this paper is thus a cooperative control architecture, blending ergonomics and compliant interaction for processing any kind of object. Indeed, by implementing the admittance control with force/torque sensor, it is possible to obtain the shaping of the inertia of the object. Thus, the proposed control strategy is suitable even for manipulating objects that are heavy and/or bulky. The presented approach uses ergonomic criteria to identify, together with an advanced perception system, the best position and orientation of the payload to maximize the ergonomics of the interaction. Furthermore, the approach integrates in a unified architecture different methods that have been adapted to interact each other. The use of the physical password to switch between different interaction modalities is implemented for the first time in a realistic and industrially relevant scenario.

This paper is organized as follows. In Section 2 the proposed strategy for ergonomic co-manipulation of payloads is presented, and in Section 3 the scheme of the control system is described. In Section 4 the proposed strategy is experimentally validated. Finally, in Section 5 some conclusions are drawn and future work is addressed.

2. Ergonomic Co-manipulation of Payloads

Consider an industrial scenario where the robot and the human have to cooperate in a shared workspace to perform different machining operations on the same workpiece. The proposed solution

https://doi.org/10.1017/S026357471900095X Published online by Cambridge University Press

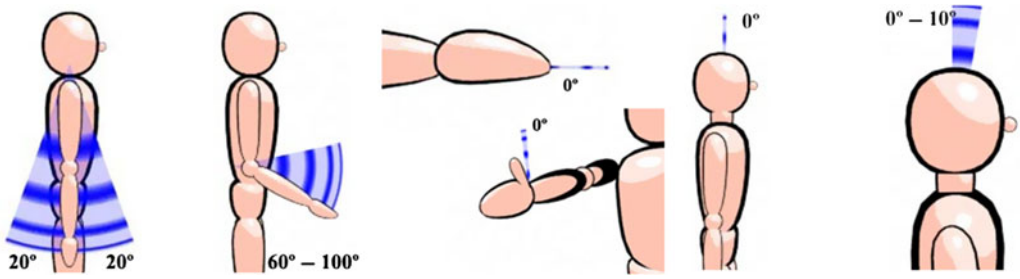


Fig. 1. Postures of the arm, the forearm, the wrist, and the neck, which are considered ergonomic according to the RULA method.

consists of two different control strategies with specific features that are integrated into a single control architecture. The system can switch between the two solutions through the identification of a predefined force pattern (called *force password*). At first a trajectory is generated so that the position-controlled robot can take the workpiece from a pallet and position it in the most comfortable position for the operator to perform the work. The trajectory is computed based on the data perceived by a vision system and on information about the ergonomics of the operation and the safety requirements. When the robot brings the object to the target point near the user location, the operator applies a predefined force pattern directly on the object. The applied force is measured by a force/torque sensor placed on the robot wrist flange, and the force password is recognized and used to activate an interaction control strategy that changes the dynamics of the object, making it light and easy to handle. This allows the operator to easily manipulate the object. An admittance control is used to obtain a compliant behavior of the system and to allow the user to safely interact with the object held by the robot. Finally, the operator moves to the position where she/he wants to work (e.g., near the tools or the devices she/he needs) and applies again the force pattern to activate the robot position control that adjusts the position of the object in order to optimize the ergonomics. Once this step has been completed, the operator restarts the machining process until it is necessary to reposition the workpiece again.

2.1. Ergonomic position control

Ergonomics is one of the key issues to be considered for a successful execution of a collaborative human–robot operation. The most important parameters for the correct human–work relation have to be identified, in order to eliminate all the negative factors that might occur, with the final goal to make the operating environment easier and more pleasant to work in.

In this work we make specific reference to the ergonomic risks associated with the postural load: quantification of such risk can be made in several ways, one of the most popular being the RULA (*Rapid Upper Limb Assessment*) method.[19] An alternative method for assessing the postural loading for both standing and sitting postures is the LUBA (*postural Loading on the Upper Body Assessment*) technique.[20] In this paper, we will apply the RULA method, which provides a practical criterion for identifying users subjected to upper limb disorders during work actions, assessing the level of risk exposure both for selected body parts and for the total body. Without going into much detail, data related to worker's postures are gathered during operations. Such postures are then compared with those reported in tables specific for selected body parts (arm, forearm, wrist, neck, trunk, and legs) obtaining partial grades, which are then combined in a final grade for the ergonomics of the worker's posture.

Despite the RULA criterion has been essentially developed for the assessment of a given posture, in this work we are rather interested in deriving a posture which satisfies some optimality in terms of minimization of the ergonomic risk. To do so, an optimal posture, corresponding to a minimum RULA level, is evaluated and the robot motion is programmed in such a way that the carried object is always offered to the human in a comfortable position for being manipulated. Figure 1 shows postures of the arm, the forearm, the wrist, and the neck, which are considered ergonomic according to the RULA method.

Based on the above considerations, the notion of an *ergonomic target point* is used in this paper. The ergonomic target point is a point, defined with respect to the operator, where the robot has to

https://doi.org/10.1017/S026357471900095X Published online by Cambridge University Press

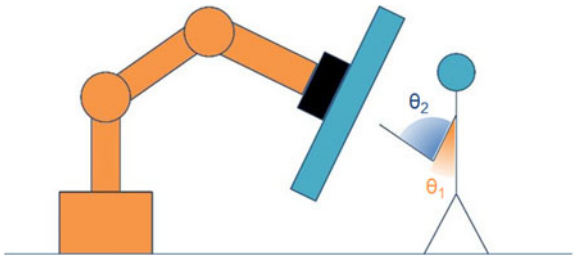


Fig. 2. Ergonomic posture of the human when operating with the robot. The angle between the arm and the vertical axis assumes the value $\theta_1 = 5°$, while the angle between the arm and the forearm is given by $\theta_2 = 95°$.

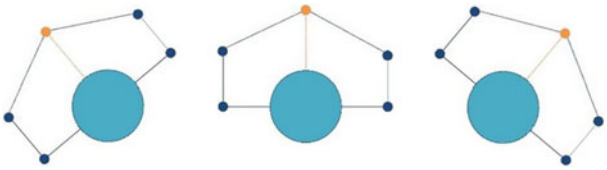


Fig. 3. Ergonomic target point with respect to the human's shoulders. The ergonomic target point is placed on a line normal to the line connecting the shoulders.

deliver the object to be manipulated, so as to guarantee ergonomics during the operations. In order to define such ergonomic target point, the angle between the arm and the vertical axis (θ_1) and the angle between the arm and the forearm (θ_2), see Fig. 2, have been assigned the values $\theta_1 = 5°$ and $\theta_2 = 95°$, respectively. Furthermore, the ergonomic target point has always been placed on a line normal to the line connecting the shoulders, see Fig. 3. The corresponding RULA index for the given posture can be evaluated to be equal to 2 in the scale that ranges from 1 to 7. A RULA index of 1 or 2 corresponds to a negligible risk that requires no specific countermeasure.

The exact point where the robot has to deliver the object depends also on the size of the object and the gripper; however, straightforward kinematic relations allow to compute such point based on the human perceived posture. In order to identify such posture, a combination of three depth cameras has been used to track selected skeletal points of the human. Sensor fusion and estimation of the points' velocities are performed through a Kalman filtering approach, described in ref. [21].

Once the target point has been online identified, the next task is to drive the robot end effector to such point making sure that all possible constraints on robot kinematics (joint position limits, joint and Cartesian maximum velocity, and acceleration), as well as possible additional constraints (e.g., related to safety), are satisfied. For this the following constrained optimization approach, adapted from ref. [22], has been used:

$$\min_{\ddot{q}_{sp}} \left(\left\| \dot{x}_{sp} - \dot{x}_{ref} \right\|^2_{Q_v} + \left\| x_{sp} - x_{ref} \right\|^2_{Q_p} \right) \tag{1a}$$

$$J\dot{q}_{sp} = \dot{x}_{sp} \tag{1b}$$

$$J\ddot{q}_{sp} + \dot{J}\dot{q}_{sp} = \ddot{x}_{sp} \tag{1c}$$

$$q^{inf} \leq q_{sp} \leq q^{sup} \tag{1d}$$

$$\dot{q}^{inf} \leq \dot{q}_{sp} \leq \dot{q}^{sup} \tag{1e}$$

$$\ddot{q}^{inf} \leq \ddot{q}_{sp} \leq \ddot{q}^{sup} \tag{1f}$$

$$-\dot{\mathcal{X}} \leq \dot{x}_{sp} \leq \dot{\mathcal{X}} \tag{1g}$$

https://doi.org/10.1017/S026357471900095X Published online by Cambridge University Press

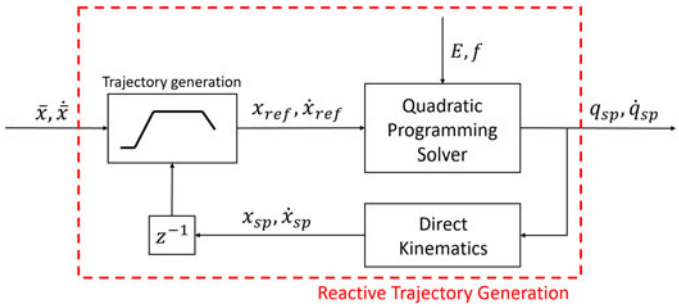


Fig. 4. Constrained optimization control scheme, adapted from ref. [22]. Given the desired position $\bar{\boldsymbol{x}}$ and its velocity $\dot{\bar{\boldsymbol{x}}}$, the Trajectory Generation block computes the best feasible set-point in the joint space which the robot must follow.

$$-\ddot{\mathcal{X}} \leq \ddot{x}_{sp} \leq \ddot{\mathcal{X}} \tag{1h}$$

$$E\ddot{q}_{sp} \leq f \tag{1i}$$

The inequalities in the constrained optimization problem are intended to be solved component-wise. The optimizer tries to minimize the tracking error with respect to a reference trajectory ($\boldsymbol{x}_{ref}$, $\dot{\boldsymbol{x}}_{ref} \in \mathbb{R}^6$), computed based on a desired position $\bar{\boldsymbol{x}} \in \mathbb{R}^6$ and velocity $\dot{\bar{\boldsymbol{x}}} \in \mathbb{R}^6$. The optimal solution is given in order to satisfy a series of constraints, ranging from the direct differential kinematics at velocity and acceleration levels (1b)–(1c) and motion limitations (1d)–(1h) to other kind of constraints, generically represented with the inequality (1i), where $\mathbf{E}$ and $\mathbf{f}$ are time-varying quantities of proper dimensions. For example, such a constraint may introduce the safety-related inequalities introduced in ref. [23], and revised in ref.[24] to account for a prediction of occupied space by the human operator. In (1b)–(1c) the term $\boldsymbol{J} \in \mathbb{R}^{6\times n}$ is the Jacobian matrix which relates the joint space to the task space. The control scheme is sketched in Fig. 4: the desired target position $\bar{\boldsymbol{x}}$, along with its velocity $\dot{\bar{\boldsymbol{x}}}$, serves as an input to a trajectory generation stage in charge of computing a trajectory from the current state of motion to the target point. A variety of methods to generate a trajectory from a given state of motion to a target one exist, see, for example, ref. [25, 26]. Their output can be made consistent with bound constraints like those in (1d)–(1h). We here assume that an algorithm for trajectory generation is available and returns the planned trajectory, in terms of desired task position and velocity. In this paper we will consider trapezoidal velocity profile trajectories. The inverse kinematics problem is implicitly solved by including in the constraints of the optimization problem the equations of the direct differential kinematics (1b)–(1c). The next state of motion is then traded off with the existing constraints (1d)–(1i), and the inverse kinematics is computed, in order to find the best feasible next state of motion in the joint space ($\boldsymbol{q}_{sp}$, $\dot{\boldsymbol{q}}_{sp} \in \mathbb{R}^n$, where n are the degrees of freedom of the robotic manipulator). This is both delivered to the low-level real time controllers and fed back in the algorithm to become, through direct kinematics, the next state of motion in Cartesian space to be used by the trajectory generator in the next iteration as a new starting point.

Let $\bar{\boldsymbol{x}}' \in \mathbb{R}^6$ be the ergonomic target position computed as previously described. When the robot has to deliver the object to the user according to the ergonomic position, the inputs of the *Trajectory Generation* block depicted in Fig. 4 are given by the ergonomic target position $\bar{\boldsymbol{x}}'$ and its velocity $\dot{\bar{\boldsymbol{x}}}'$.

2.2. Admittance control with payload compensation

Since the safety of the human operator during her/his work on the object held by the robot is a primary concern, compliant control strategies have to be implemented when the user interact with the robot. Impedance and admittance control[7] are used to modify the robot dynamics, according to a mass-spring-damper model with tunable parameters. While impedance control is more suitable for backdrivable robots, admittance control is used for stiff and non-backdrivable robots, as the industrial ones.

https://doi.org/10.1017/S026357471900095X Published online by Cambridge University Press

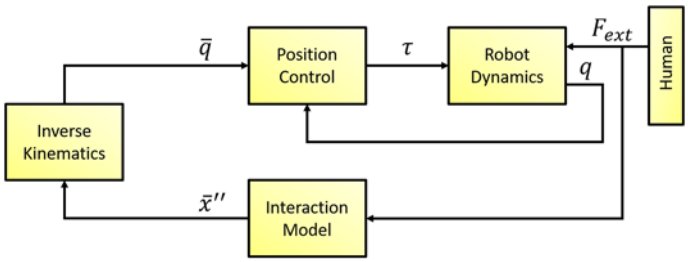


Fig. 5. Control scheme of the admittance control with underlying motion controller. The interaction model (3) with the input $\boldsymbol{F}_{ext}$ is solved by using the single Euler integrator in order to provide the value $\bar{\boldsymbol{x}}''$ which the position-controlled robot must follow.

Consider an n-degrees of freedom manipulator controlled by using the admittance control shown in Fig. 5. Given a desired interaction model, namely a dynamic relation between the motion of the robot and the force applied by the environment, and given the external force, the admittance equation, via a suitable integration, generates the reference pose for the low-level position controller. Let $\bar{\boldsymbol{x}}''$, $\boldsymbol{x} \in \mathbb{R}^6$ be the set-point computed by the admittance controller and the pose of the end-effector, respectively. As suggested in ref. [27], we will assume that the robot can track a feasible set-point, that is, we will make the following assumption:

Assumption 1. *The low-level position controller is designed and tuned in such a way that* $\boldsymbol{x} \simeq \bar{\boldsymbol{x}}''$ *as long as*

$$-\dot{\mathcal{X}} \leq \dot{\bar{x}}'' \leq \dot{\mathcal{X}} \qquad -\ddot{\mathcal{X}} \leq \ddot{\bar{x}}'' \leq \ddot{\mathcal{X}} \tag{2}$$

where $\dot{\mathcal{X}}, \ddot{\mathcal{X}} \in \mathbb{R}^6$ *are velocity and acceleration bounds due to the robot dynamics and the inequalities are component-wise.*

We consider a scenario where the human operator can directly manipulate the object held by the robot applying a force to the object itself and thus to the end-effector. Therefore, we do not consider elastic terms in the admittance control model,[7] and we aim at controlling the robot to behave according to the following desired behavior:

$$\boldsymbol{M}_d \ddot{\boldsymbol{x}} + \boldsymbol{D}_d \dot{\boldsymbol{x}} = \boldsymbol{F}_{ext} \tag{3}$$

where $\boldsymbol{M}_d$, $\boldsymbol{D}_d \in \mathbb{R}^{6\times 6}$ are, respectively, the desired inertia and damping symmetric and positive definite matrices. The external force $\boldsymbol{F}_{ext} \in \mathbb{R}^6$ is assumed to be measured by a 6-DOF force/torque (F/T) sensor attached at the robot wrist flange. Since the object to be worked is held by the robot end-effector, the measured forces and torques are affected by its static components (i.e., weight) and the dynamic ones (i.e., inertial, centrifugal/Coriolis). The magnitude of these noncontact forces is proportional to the acceleration during the movement of the object, modifying the desired dynamics and deteriorating the performance. In this scenario the measured forces $\boldsymbol{F}_{ext}$ embody both the contact forces $\boldsymbol{F}_c$, produced by the human–robot interaction, and the noncontact ones $\boldsymbol{F}_{nc}$ that are due to the payload and have to be computed and eliminated. Following the strategy proposed in ref. [11], the static and dynamic effects of the object held by the robot can be compensated implementing a tool compensation algorithm. The algorithm requires the knowledge of the robot linear acceleration $\hat{\boldsymbol{a}}$, angular acceleration $\hat{\boldsymbol{\alpha}}$, and angular velocity $\hat{\boldsymbol{\omega}}$. These data can be estimated by using Kalman filters starting from the current pose of the robot end-effector $\boldsymbol{x}$, as suggested in ref. [28].

In order to compensate the static and dynamic effects of the object held by the robot end-effector, it is required to relate the dynamics of the tool and its inertial parameters, that is, mass, center of mass, and inertia tensor, with the forces/torques measured by the F/T sensor. Even if the dynamic parameters may be calibrated online, as described in ref. [29], we consider that in a typical industrial application the properties of the workpiece are known in advance. The noncontact forces/torques $\boldsymbol{F}_{nc} = \left[\boldsymbol{f}_{nc}\, \boldsymbol{\tau}_{nc}\right]$ can be computed, according to the Newton–Euler formulation and to the motion of a rigid body due to external forces and torques, as follows:

$$\boldsymbol{F}_{nc} = \boldsymbol{V}(\boldsymbol{a}, \boldsymbol{\alpha}, \boldsymbol{\omega}, \boldsymbol{g})\boldsymbol{\varphi} \tag{4}$$

https://doi.org/10.1017/S026357471900095X Published online by Cambridge University Press

where $\boldsymbol{V}(\boldsymbol{a}, \boldsymbol{\alpha}, \boldsymbol{\omega}, \boldsymbol{g})$ is a 6×10 matrix whose elements depend on the linear acceleration $\boldsymbol{a}$, on the angular velocity and acceleration $\boldsymbol{\omega}$ and $\boldsymbol{\alpha}$ and on the gravity vector $\boldsymbol{g}$, while $\boldsymbol{\varphi}$ is the load inertial vector, which is defined as:

$$\boldsymbol{\varphi} = [m, mc_x, mc_y, mc_z, I_{xx}, I_{xy}, I_{xz}, I_{yy}, I_{yz}, I_{zz}]^T \tag{5}$$

being m the mass of the object, $\boldsymbol{c} = \left[c_x, c_y, c_z\right]$ its center of mass and $\boldsymbol{I}$ the 3×3 inertia tensor. Further details can be found in ref. [12].

Equation (4) does not consider the sensor offset and the thermal drift on forces and torques typical of strain gauge-based devices.[30] The measurements change with temperature variation, until the steady state is reached, deteriorating the performance as result. For this reason the device has to be periodically zeroed using a tare function embedded in the sensor. Since the object held by the robot could be heavy or bulky, it cannot be easily detached from the end-effector. In this case, force and torques of the offset term can still be eliminated with the help of (4). Indeed, the loaded F/T sensor can be zeroed in a static initial condition with a known orientation, and the following *pseudo-gravitational* term can be added to subsequent readings to eliminate the gravitational forces and the associated torques:

$$\boldsymbol{F}_{g_{init}} = \boldsymbol{V}(\boldsymbol{0}, \boldsymbol{0}, \boldsymbol{0}, \boldsymbol{g_{init}})\boldsymbol{\varphi} \tag{6}$$

This offset zeroing operation should also be repeated periodically, during a pause of the robotic task, to cope with temperature variations and slow drifts.

Since perfect knowledge of the inertial parameters cannot be achieved and there could be estimation errors of the Kalman filter, the computation of contact forces/torques is based on uncertain quantities. These uncertainties can be compensated by applying threshold-based logics as, for example, the one provided in ref. [28]. Therefore, the expression of contact forces/torques can be written as follows:

$$\hat{\boldsymbol{F}}_c = \boldsymbol{F}_{ext} - \hat{\boldsymbol{F}}_{nc} + \hat{\boldsymbol{F}}_{g_{init}} \tag{7}$$

The estimated contact forces/torques are provided as input to the admittance control instead of the measured forces/torques. In this way, the reference set-point computed by the admittance control allows to track the human motion, independently of the noncontact forces/torques due to the payload held by the robot end-effector.

When the admittance control is activated in the unified architecture, the admittance set-point $\bar{\boldsymbol{x}}''$, along with its velocity $\dot{\bar{\boldsymbol{x}}}''$, serves as input to the *Trajectory Generation* block shown in Fig. 4 that computes, according to (1), the best feasible set-point in the joint space to be delivered to the low-level robot controller.

2.3. Triggering the switch between controls

The systems described in Sections 2.1 and 2.2 are used in the overall control architecture for different purposes. In particular, the ergonomic position control (Section 2.1) is used for positioning the object in the most comfortable position for the user, while the admittance control with payload compensation (Section 2.2) allows the user to easily move the object for subsequent working operations.

The contact force estimated in (7) is used for triggering the switch between the two systems. Indeed, a force pattern identification can be implemented. In this work we have exploited the strategy proposed in ref. [31]. In this way, the robot will place the object in the ergonomic position and, without any need of external buttons or remote control, the operator can apply the force password to the object. A force supervisor component manages the pattern identification for commanding the switch to the admittance control.

3. Proposed Control Architecture

The overall control scheme of the proposed system is shown in Fig. 6. As described in Section 2, the system includes two different control strategies for computing the reference pose $\bar{\boldsymbol{x}}$ that the robot must follow:

https://doi.org/10.1017/S026357471900095X Published online by Cambridge University Press

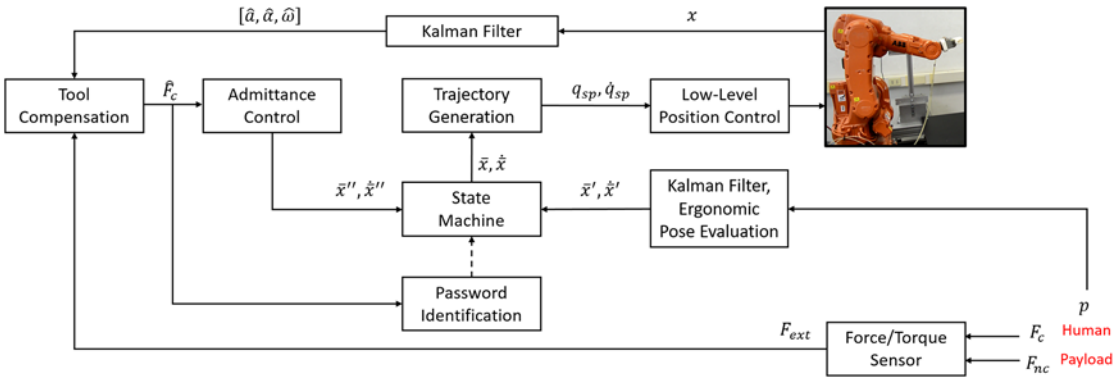


Fig. 6. The overall control scheme of the proposed system.

- The ergonomic target point $\bar{\boldsymbol{x}}'$ is computed in order to offer the object to the user in such a way that the human posture is considered to be ergonomic, as described in Section 2.1. The human posture is identified using depth cameras that track the selected skeletal points $\boldsymbol{p}$ of the human.
- The compliant set-point $\bar{\boldsymbol{x}}''$ is computed to allow the user to easily manipulate the object. The admittance control requires as input the contact forces/torques computed as described in Section 2.2.

The choice of the set-point $\bar{\boldsymbol{x}}$ to be provided to the robot is performed by a state machine on the basis of the force password identified using the strategy described in Section 2.3. The selected set-point constitutes the input $\bar{\boldsymbol{x}}$ of the Reactive Trajectory Generation block shown in Fig. 4 that computes the best feasible position in the joint space according to the constrained optimization problem formalized in (1). The joint positions $\bar{\boldsymbol{q}}_{sp}$ are the set-points that the position-controlled robot must follow.

Both the admittance control and the password identification component require as input the estimated contact forces/torques $\hat{\boldsymbol{F}}_c$. These forces/torques are computed through the tool compensation algorithm described in Section 2.2 starting from the forces/torques $\boldsymbol{F}_{ext}$ measured by a 6 axis F/T sensor. The algorithm requires the knowledge of the robot linear acceleration $\hat{\boldsymbol{a}}$, angular acceleration $\hat{\boldsymbol{\alpha}}$ and angular velocity $\hat{\boldsymbol{\omega}}$ that are estimated by a Kalman filter starting from the current pose of the robot end-effector $\boldsymbol{x}$.

4. Experimental Results

The proposed control architecture has been implemented in a setup including an ABB IRB 140 industrial robot, equipped with a 6 axis Robotiq FT300 F/T sensor. The tracking of the human body and the computation of the ergonomic point is performed analyzing data coming from an ASUS Xtion. The software components have been developed using Simulink and the Orocos framework, and they run with a 250 Hz frequency. The operator has to perform operations on the back of the control panel of an oven that is held by the robot end-effector. In particular, the panel is $50 \times 10 \times 3$ cm long and its mass is 1.5 kg. The experimental setup is shown in Fig. 7 where the reference frame for the robot end-effector is also reported. We performed two different experiments:

- The first experiment (Section 4.1) aims at showing in detail the functionalities of the proposed control strategy and, in particular, of the different subsystems.
- In the second experiment (Section 4.2) we considered a practical case to evaluate the overall architecture. We asked 10 users to perform the experiment, with and without the proposed control system, and we compared the results.

4.1. Validation of the proposed control strategy

In this experiment, the robot moves from a starting position to an ergonomic target position in front of the human operator. The position of the human body is tracked and the ergonomic target point that serves as the set-point for the low-level position control is computed according to the methodology described in Section 2.1. Then, if the operator moves, the ergonomic control updates the ergonomic target position accordingly.

https://doi.org/10.1017/S026357471900095X Published online by Cambridge University Press

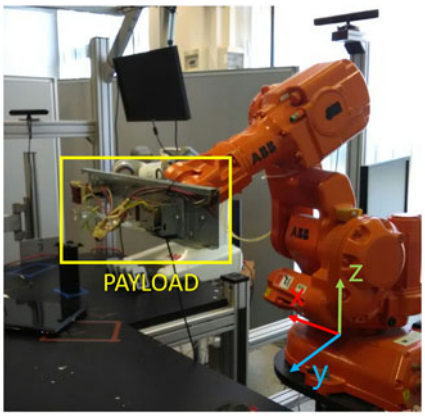


Fig. 7. Experimental setup used to validate the proposed control system.

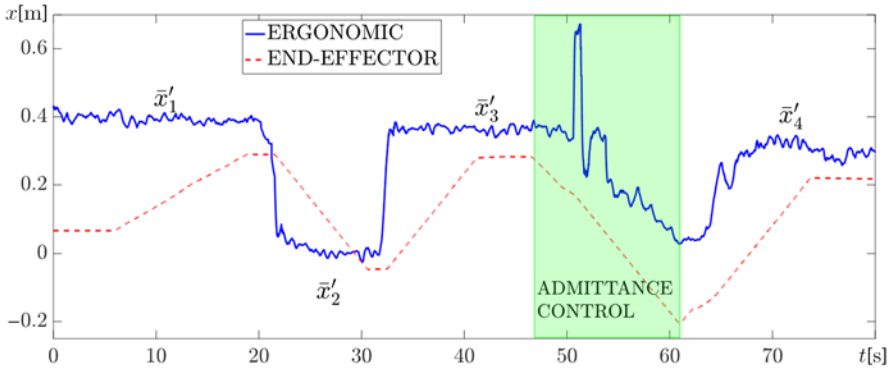


Fig. 8. Evolution over time of the ergonomic position along x axis (blue solid line) computed by the ergonomic pose evaluator and of the end-effector position (dashed red line).

As shown in Fig. 8, the ergonomic control computes four different ergonomic positions (denoted as $\bar{x}'_1, \ldots, \bar{x}'_4$ and corresponding to the blue trajectory) consistent with the operator movements, and the robot tracks the target points consequently. The movement of the robot end-effector is depicted with a dashed red line. For clarity of presentation, we reported the positions only along the x direction, but similar behaviors have been observed along the other directions. The ergonomic target point is positioned on the object attached at the robot end-effector. This results in an offset with respect to the end-effector reference system that can be clearly seen in Fig. 8 as a translation between the two trajectories. When the robot switches to admittance control, the end-effector of the robot tracks the force applied by the human operator according to Section 2.2, resulting in a different trajectory (time interval: [55.2; 70.8] s). In this period of time the human operator skeletal points are still tracked by the depth camera to keep the ergonomic point updated even if the reference set-point is given by the admittance control.

In particular, if the human operator wants to move the object to a new position by switching to the admittance control mode, she/he can apply the force password on the object. Hence the control system recognizes it and switches from the ergonomic position control to the admittance control with payload compensation described in Section 2.2. In particular, the user inserts the password by applying a repetition of four torque values (greater than 2 Nm), alternatively positive and negative, around the y axis. This value has been experimentally determined and it is suitable for the task being performed. However, both the value and the force/torque pattern can be arbitrarily selected depending on the task and/or the operator. When the operator has finished the object's manipulation, she/he repeats the password and the control system switches back to the ergonomic position control which computes and tracks the ergonomic target point for the new human pose. Figure 9 shows an example of profile of the torque around the y-axis when inserting the force password.

https://doi.org/10.1017/S026357471900095X Published online by Cambridge University Press

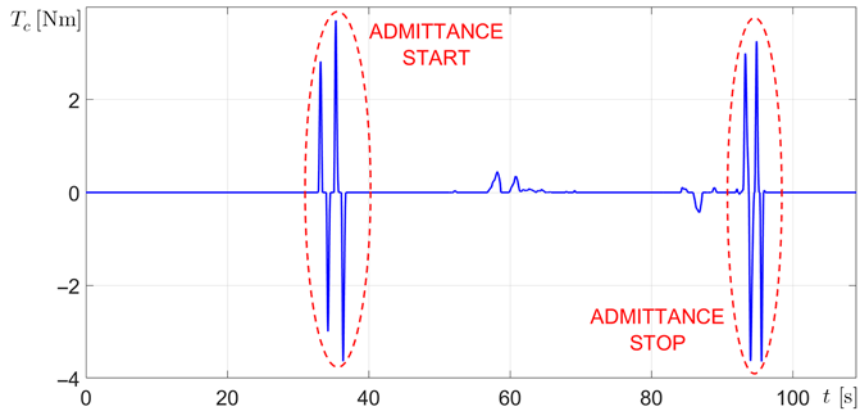


Fig. 9. Password detection allowing the switch between ergonomic position control and admittance control and vice versa. Torque around the y axis.

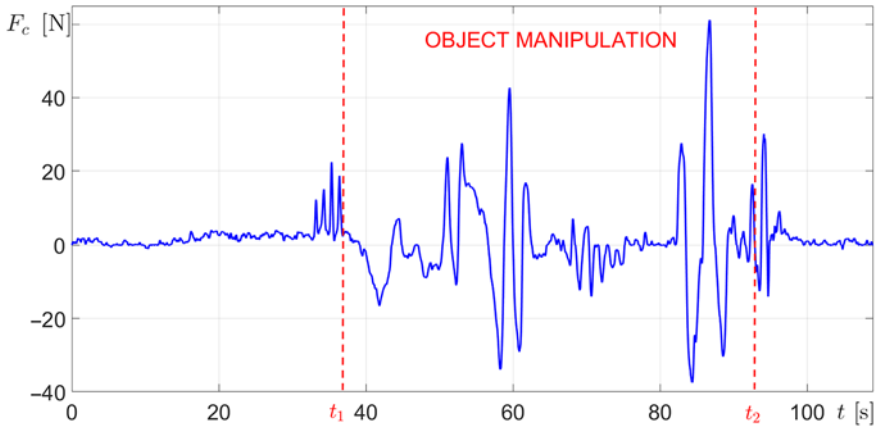


Fig. 10. Estimated contact force along z direction.

During the manipulation of the object performed by the user, the robot is admittance-controlled. After several experiments to evaluate the best human feeling during the interaction, inertia and damping parameters have been empirically tuned and chosen as constant diagonal matrices with inertia 1.4 kg and 0.8 kg/m^2 for the translational and rotational parts, respectively, and damping 160 Ns/m and 8 Nms/rad for the translational and rotational parts, respectively. The interaction force is the only input to the admittance control, and thus the smoother the F/T profile is, the smoother the robot motion will be. As previously described, the noncontact wrench is due to the tool mass, inertia, Coriolis, and centrifugal terms, and it has to be subtracted from the one measured by the sensor to obtain the estimated contact forces/torques, which are shown in Fig. 10. Figure 10 reports plots of the robot behavior along the z-axis, since in this direction the contribution of the noncontact forces can be clearly understood. Indeed, the noncontact force along the z direction includes, for example, a significant contribution due to the gravity. This contribution would greatly affect the estimated contact forces/torques if the compensation is not applied. Figure 10 highlights that in the time interval between the two password insertions ($t \in [t_1; t_2]$) when the admittance control is active, the user is actually manipulating the object and the contact forces are significant. In the remaining time intervals ($t < t_1$ and $t > t_2$), the user does not interact with the object since the robot is position-controlled and the forces are near to zero. The remaining forces are due to the noise of the F/T sensor.

4.2. Evaluation in a practical scenario

In the second experiment, a practical scenario is implemented where the use of the overall architecture is emphasized. Moreover, a comparison of the execution of the experiment with and without the proposed control strategy is provided. An accompanying video clip that shows the experiment described in the following can be found at the link https://streamable.com/ir2yo. Suppose that the

https://doi.org/10.1017/S026357471900095X Published online by Cambridge University Press

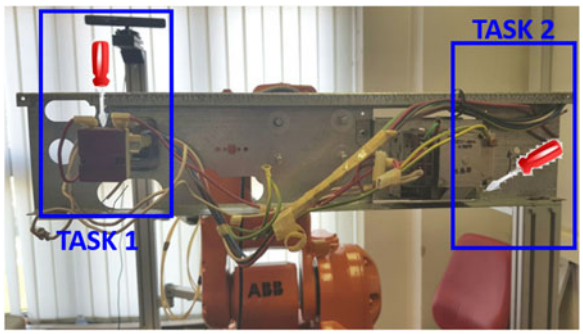


Fig. 11. The part to be worked is the back of the control panel of an oven. The operator has to tighten the screws of the control panel in two different positions (task 1 and task 2).

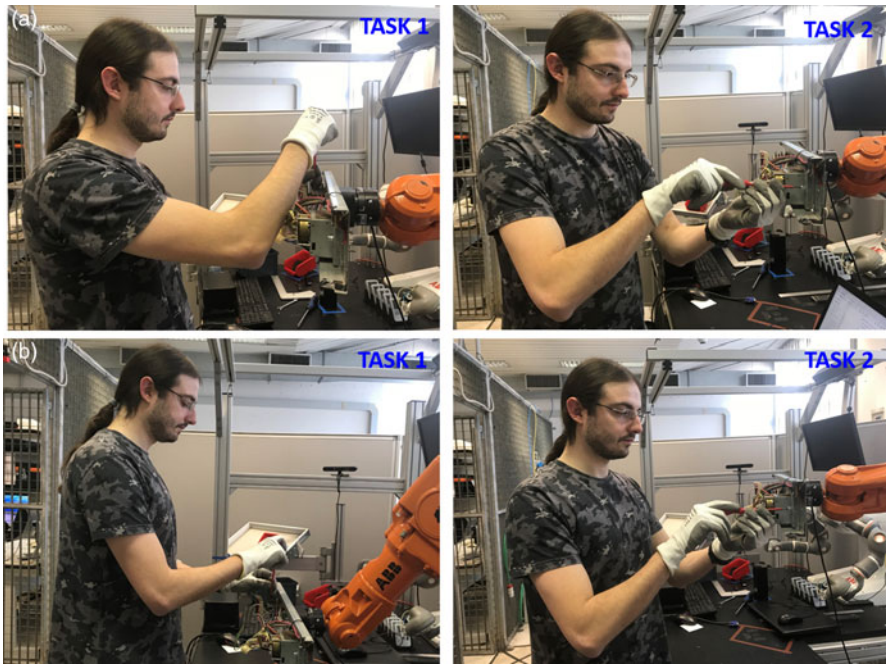


Fig. 12. Postures assumed by the operator during the execution of the two tasks.

operator has to tighten the screws of the control panel in two different positions, denoted as *task 1* and *task 2* in Fig. 11. In a first implementation using the standard techniques (e.g., only position control for pick and place), the robot is used to take the control panel from a pallet and to bring it in front of the operator, in a fixed target position. Depending on where the operations have to be performed on the piece, the operator could assume uncomfortable postures. For example, as shown in Fig. 12(a) task 1 is performed by the operator with a very large angle between the arm and the vertical axis (i.e., θ_1 in Fig. 2) which is considered to be not ergonomic according to the RULA method.

Then, the control strategy proposed in this paper has been implemented and the following steps have been performed. Figure 13 shows the trajectory executed by the end-effector of the robot in each step.

1. The robot moves the object to the most comfortable position for the operator to perform the work, according to the theory of Section 2.1 (time interval: [0.0; 23.1] s).
2. The operator performs task 1 while the robot keeps holding the object (time interval: [23.2; 46.9] s).
3. The operator notices that having the object in a higher position would be more comfortable to perform the task 2. Thus, she/he applies the force password at $t = 47.0$ s and move the object to

https://doi.org/10.1017/S026357471900095X Published online by Cambridge University Press

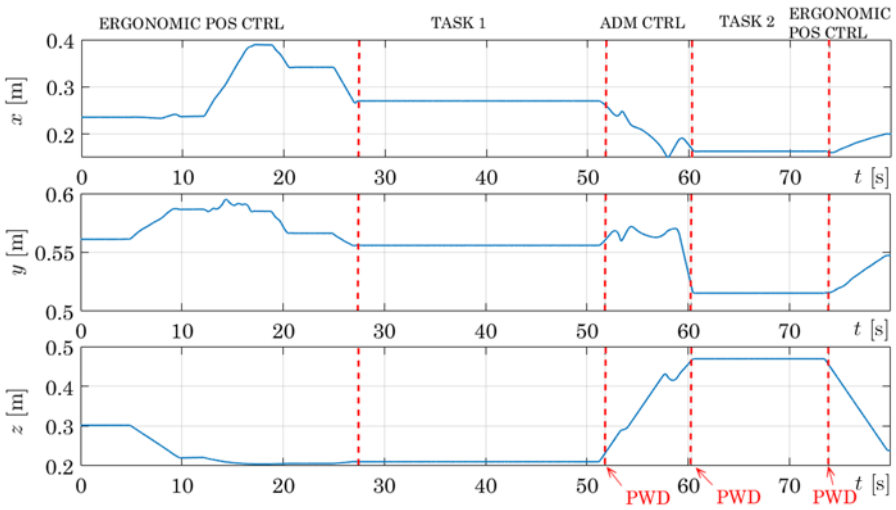


Fig. 13. Trajectory executed by the robot end-effector while performing the described experiment.

the preferred position. The object is easy to be moved, since the robot is compliant and admittance-controlled (time interval: [47.0; 56.3] s).

4. When the desired position is reached, the operator can reinsert the force password at $t = 56.4$ s and the robot stops in that position. The operator performs the task 2 (time interval: [56.4; 69.2] s).
5. After the second task, the operator applies again the force password at $t = 69.3$ s, and the robot switches to the ergonomic position control to move the object in the most comfortable position for the operator (time interval: from $t = 69.4$ s to the end of the experiment).

As shown in Fig. 12(b), the proposed strategy allows the operator to take an ergonomic posture when executing both tasks. Figure 14(a) shows the forces measured by the F/T sensor during the experiment, while Fig. 14(b) shows the estimated contact forces computed applying the strategy described in Section 2.2: they are smooth and damped, leading to a stable end-effector behavior. Indeed, since the human force interaction is the only input in the system, the smoother is the F/T profile, the smoother will be the robot motion. As described in Section 2.2, the noncontact forces (Fig. 14(c)) are due to the tool mass, inertia, Coriolis, and centrifugal terms, and they have to be subtracted from the sensor measured forces to obtain the estimated contact ones.

Finally, a qualitative evaluation has been obtained asking 10 users to fill the questionnaire for Physical Assistive Devices (QUEAD) proposed in ref. [32], including a total of 13 statements, to be scored with a number from 1 (entirely disagree) to 7 (entirely agree), and related to five aspects of the human–robot interaction: usefulness, ease of use, emotions, attitude, and comfort. The set of users considered in our experiments was composed of people between the age of 20 and 35, 8 males and 2 females. The questionnaire is shown in Table I. Users were instructed to refer their evaluation to the proposed control strategy, and also to give their preference regarding the experiment with and without the proposed system. Table II reports the results of the questionnaire for each of the five aspects and shows that the qualitative evaluations are always higher than 4.40 out of maximum level of 7 on all features. In particular, three of them (usefulness, emotions, and attitude) reported evaluations higher than 5.07, which lead optimistically towards a future implementation of the proposed control strategy in a real industrial setup. Moreover, all the 10 users selected the proposed control strategy as preferred control modality with respect to the standard method (no active control).

5. Conclusions and Future Works

In this paper, we have proposed a safe and ergonomic architecture for human–robot co-manipulation of objects of different shape and weight, including heavy and/or bulky ones. The robot capabilities have been combined to the user's skills to create a system where the robot carries and holds the object, while the human operator manipulates it and performs the required work.

The proposed architecture consists of two working modes that are activated in a mutually exclusive way: an ergonomic planner has been developed to compute the target point for the low-level robot

https://doi.org/10.1017/S026357471900095X Published online by Cambridge University Press

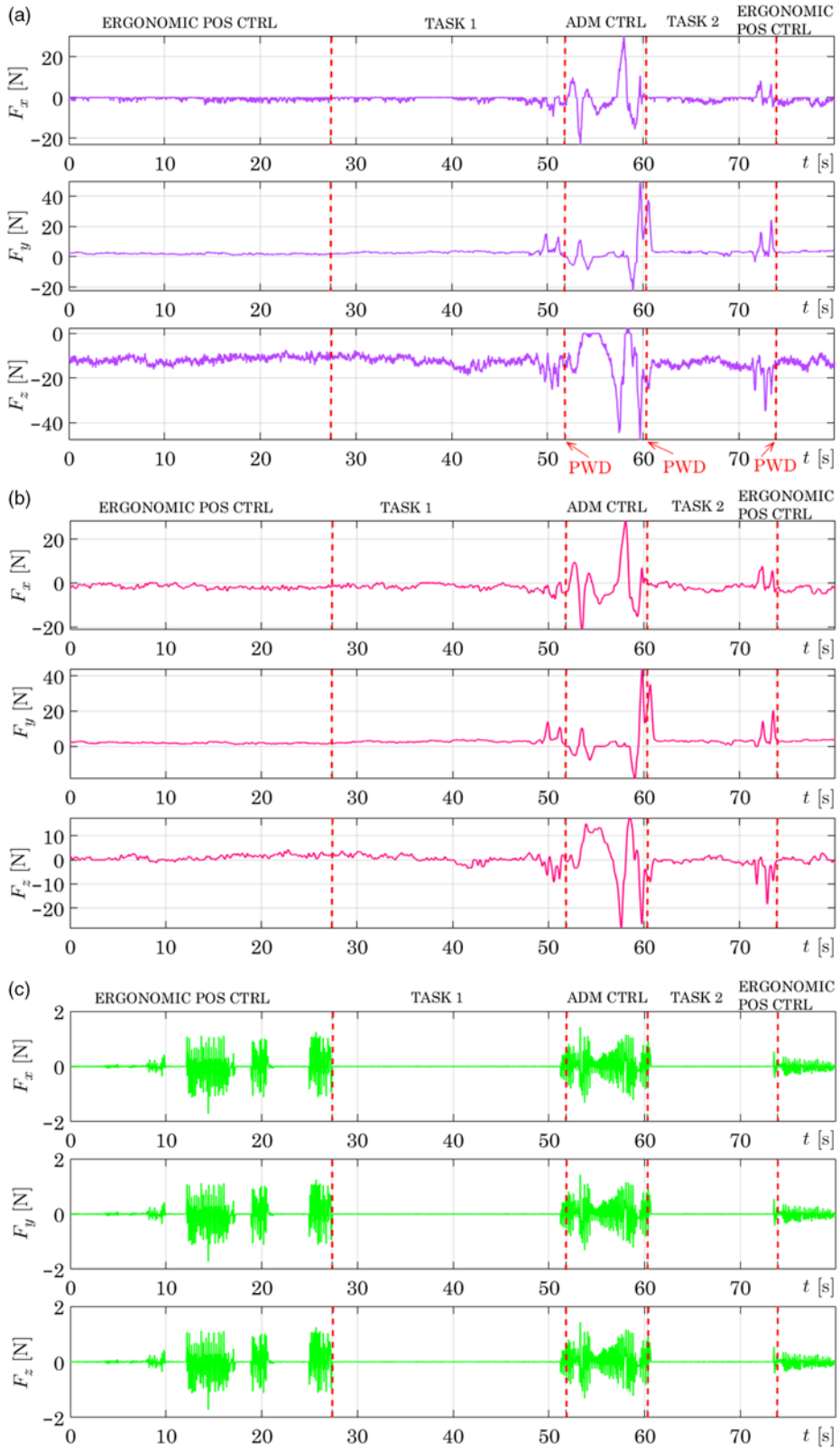


Fig. 14. Measured and estimated forces during the whole experiment.

controller in order to offer the object to the human operator in a way that the human posture is considered to be ergonomic, while an admittance control with payload compensation is used to allow the operator to easily manipulate the part, while working on it. The switch between the two working

https://doi.org/10.1017/S026357471900095X Published online by Cambridge University Press

Table I. Questionnaire proposed to the users. Each item can be evaluated from 1 (Disagree) to 7 (Agree).

Perceived usefulness	PU1	The control mode is useful
	PU2	The control mode enhances my working performance
	PU3	I accomplished the given task rapidly
Perceived ease of use	PEU1	This control mode is easy to use
	PEU2	This control mode feels cumbersome
	PEU3	This control mode would be helpful to me
	PEU4	It was easy to learn to use the control mode
Emotions	E1	I like using this control mode
	E2	I feel comfortable using this control mode
	E3	I feel anxious using this control mode
Attitude	A1	I think that using this control mode is a good idea
Comfort	C1	I feel physically uncomfortable in using this control mode
	C2	I feel tense in using this control mode

Table II. Results of qualitative evaluations with QUEAD[32] (1: Disagree; 7: Agree).

Usefulness	Ease of use	Emotions	Attitude	Comfort
5.43	4.88	5.07	5.50	4.40

modes is implemented by means of a force password which saves the user from taking care of external interfaces.

Future work aims at rendering the overall architecture compliant with the current international regulations on safety in order to implement the proposed system in a real industrial setup, with heavy and bulky objects provided by the company itself. Moreover, we aim at performing a detailed usability analysis related to the force pattern, in order to find the most suitable pattern or force/torque value to be used for each operator. Finally, we will perform the usability analysis on workers working at the industrial site.

Acknowledgments

This work was supported by the project ADAPTIVE (CTN01_00163_216730), funded by the Italian Ministry of education, university and research, and by the University of Bergamo.

References

1. N. Pedrocchi, M. Malosio and L. Molinari Tosatti, "Safe Obstacle Avoidance for Industrial Robot Working Without Fences," *Proceedings of the IEEE International Conference on Intelligent Robots and Systems*, St. Louis, MO, USA (2009) pp. 3435–3440.
2. R. Meziane, M. J.-D. Otis and H. Ezzaidi, "Human-robot collaboration while sharing production activities in dynamic environment: SPADER system," *Robot. Comput.-Integr. Manuf.* **48**, 243–253 (2017).
3. M. Hagele, W. Schaaf and E. Helms, "Robot Assistants at Manual Workplaces: Effective Co-operation and Safety Aspects," *Proceedings of the International Symposium on Robotics*, Washington, DC, USA (2002).
4. A. De Santis, B. Siciliano, A. De Luca and A. Bicchi, "Atlas of physical human-robot interaction," *Mech. Mach. Theory*. **43**(3), 253–270 (2008).
5. J. Kruger, T. K. Lien and A. Verl, "Cooperation of human and machines in assembly lines," *CIRP Ann. Manuf. Technol.* **58**(2), 628–646 (2009).
6. R. D. Schraft, M. Hagele and A. Breckweg, "Man and robot without separating systems," **In**: *World of Automation and Metalworking*, Frankfurt/M (2006).
7. L. Villani and J. De Schutter, "Force control," **In**: *Springer Handbook of Robotics* (B. Siciliano and O. Khatib, eds.) (Springer, Berlin Heidelberg, 2008).
8. L. Bascetta, G. Ferretti, G. Magnani and P. Rocco, "Walk-through programming for robotic manipulators based on admittance control," *Robotica* **31**(7), 1143–1153 (2013).
9. V. Duchaine and C. Gosselin, "Safe, Stable and Intuitive Control for Physical Human-robot Interaction," *Proceedings of the IEEE International Conference on Robotics and Automation*, Kobe, Japan (2009) pp. 3383–3388.
10. K. Kosuge and N. Kazamura, "Control of a Robot Handling an Object in Cooperation with a Human," *Proceedings of the IEEE International Workshop on Robot and Human Communication*, Sendai, Japan (1997) pp. 142–147.
11. D. Kubus, T. Kröger and F. Wahl, "Improving Force Control Performance by Computational Elimination of Non-contact Forces/Torques," *Proceedings of the IEEE International Conference on Robotics and Automation*, Pasadena, USA (2008) pp. 2617–2622.

https://doi.org/10.1017/S026357471900095X Published online by Cambridge University Press

12. C. Talignani Landi, F. Ferraguti, C. Secchi and C. Fantuzzi, "Tool Compensation in Walk-Through Programming for Admittance-Controlled Robots," *Proceedings of the Annual Conference of IEEE Industrial Electronics Society*, Firenze, Italy (2016).
13. A. M. Bestick, S. A. Burden, G. Willits, N. Naikal, S. S. Sastry and R. Bajcsy, "Personalized Kinematics for Human-robot Collaborative Manipulation," *Proceedings of the IEEE/RSJ International Conference on Intelligent Robots and Systems*, Hamburg, Germany (2015) pp. 1037–1044.
14. N. Hu, A. Bestick, G. Englebienne, R. Bajscy and B. Kröse, "Human Intent Forecasting using Intrinsic Kinematic Constraints," *Proceedings of the IEEE/RSJ International Conference on Intelligent Robots and Systems*, Daejeon, South Korea (2016) pp. 787–793.
15. W. Kim, J. Lee, L. Peternel, N. Tsagarakis and A. Ajoudani, "Anticipatory robot assistance for the prevention of human static joint overloading in human-robot collaboration," *IEEE Robot. Autom. Lett.* **3**(1), 68–75 (2018).
16. O. Karhu, P. Kansi and I. Kuorinka, "Correcting working postures in industry: A practical method for analysis," *Appl. Ergon.* **8**(4), 199–201 (1977).
17. G. I. Lee, M. R. Lee, T. Clanton, E. Sutton, A. E. Park and M. R. Marohn, "Comparative assessment of physical and cognitive ergonomics associated with robotic and traditional laparoscopic surgeries," *Surg. Endosc.* **28**(2), 456–465 (2014).
18. W. Bauer, M. Bender, P. Rally, O. Scholtz and M. Hämmerle, *Lightweight Robots and Human Interaction in Assembly Systems* (Springer International Publishing, Cham, 2016) pp. 113–122.
19. L. McAtamney and E. N. Corlett, "Rula: a survey method for the investigation of work-related upper limb disorders," *Appl. Ergon.* **24**(2), 91–99 (1993).
20. D. Kee, and W. Karwowski, "LUBA: An assessment technique for postural loading on the upper body based on joint motion discomfort and maximum holding time," *Appl. Ergon.* **32**, 357–366 (2001).
21. F. De Groote, T. De Laet, I. Jonkers and J. De Schutter, "Kalman smoothing improves the estimation of joint kinematics and kinetics in marker-based human gait analysis," *J. Biomech.* **41**(16), 3390–3398 (2008).
22. A. M. Zanchettin and P. Rocco, "Motion planning for robotic manipulators using robust constrained control," *Control Eng. Prac.* **59**, 127–136 (2017).
23. A. M. Zanchettin, N. M. Ceriani, P. Rocco and B. Matthias, "Safety in human-robot collaborative manufacturing environments: metrics and control," *IEEE Trans. Autom. Sci. Eng.* **13**(2), 882–893 (2016).
24. M. Ragaglia, A. M. Zanchettin and P. Rocco, "Trajectory generation algorithm for safe human-robot collaboration based on multiple depth sensor measurements," *IFAC Mechatronics* **55**, 267–281 (2018).
25. L. Biagiotti and C. Melchiorri, *'Trajectory Planning for Automatic Machines and Robots* (Springer, Berlin Heidelberg, 2008).
26. T. Kroeger and F. Wahl, "Online trajectory generation: basic concepts for instantaneous reactions to unforeseen events," *IEEE Trans. Robot.* **26**, 94–111 (2010).
27. C. Talignani Landi, F. Ferraguti, L. Sabattini, C. Secchi, M. Bonfè and C. Fantuzzi, "Variable Admittance Control Preventing Undesired Oscillating Behaviors in Physical Human-robot Interaction," *Proceedings of the IEEE International Conference on Intelligent Robots and Systems*, Vancouver, Canada (2017).
28. S. Farsoni, C. Talignani Landi, F. Ferraguti, C. Secchi and M. Bonfè, "Compensation of load dynamics for admittance controlled interactive industrial robots using a quaternion-based kalman filter," *IEEE Robot. Autom. Lett.* **2**(2), 672–679 (2017).
29. D. Kubus, T. Kröger and F. Wahl, "On-line Estimation of Inertial Parameters using a Recursive Total Least-Squares Approach," *Proceedings of the IEEE/RSJ International Conference on Intelligent Robots and Systems*, Nice, France (2008).
30. R. M. Voyles Jr, J. D. Morrow and P. K. Khosla, "A comparison of force sensors," *Advanced manipulators laboratory, the Robotic Institute Carnegie Mellon University* (1994).
31. C. Talignani Landi, F. Ferraguti, C. Secchi and C. Fantuzzi, "Tool Compensation and Force Password Identification on Admittance-Controlled Robots in Walk-Through Programming," *9th International Workshop on Human Friendly Robotics*, Genoa, Italy (2016).
32. J. Schmidtler, K. Bengler, F. Dimeas and A. Campeau-Lecours, "A questionnaire for the evaluation of physical assistive devices (quead)," *IEEE International Conference on Systems, Man and Cybernetics (SMC)*, Canada (2017) pp. 876–881.

https://doi.org/10.1017/S026357471900095X Published online by Cambridge University Press